Low-Molecular-Weight Peptidic and Cyclic Antagonists of the Receptor for the Complement Factor C5a

Angela M. Finch,[†] Allan K. Wong,[‡] Natalii J. Paczkowski,[†] S. Khémar Wadi,[†] David J. Craik,[‡] David P. Fairlie,[‡] and Stephen M. Taylor*,[†]

Department of Physiology and Pharmacology and Centre for Drug Design and Development, University of Queensland, Brisbane, Queensland 4072, Australia

Activation of the human complement system of plasma proteins during immunological host defense can result in overproduction of potent proinflammatory peptides such as the anaphylatoxin C5a. Excessive levels of C5a are associated with numerous immunoinflammatory diseases, but there is as yet no clinically available antagonist to regulate the effects of C5a. We now describe a series of small molecules derived from the C-terminus of C5a, some of which are the most potent low-molecular-weight C5a receptor antagonists reported to date for the human polymorphonuclear leukocyte (PMN) C5a receptor. ¹H NMR spectroscopy was used to determine solution structures for two cyclic antagonists and to indicate that antagonism is related to a turn conformation, which can be stabilized in cyclic molecules that are preorganized for receptor binding. While several cyclic derivatives were of similar antagonistic potency, the most potent antagonist was a hexapeptide-derived macrocycle AcF[OPdChaWR] with an IC_{50} = 20 nM against a maximal concentration of C5a (100 nM) on intact human PMNs. Such potent C5a antagonists may be useful probes to investigate the role of C5a in host defenses and to develop therapeutic agents for the treatment of many currently intractable inflammatory conditions.

Introduction

During host defense the complement system of plasma proteins initiates inflammatory and cellular responses to stimuli such as infectious microorganisms (bacteria, viruses, parasites), chemical and physical injury, radiation, or neoplasia. Prolonged activation of the human complement system results in elevated C5a levels that are associated with numerous diseases including rheumatoid arthritis,[1] Alzheimer's disease,[2] ischemic heart disease,[3] and adult respiratory distress syndrome (ARDS).[4] At present there is no clinically available antagonist to combat the effects of C5a in disease development.

C5a receptor (C5aR) antagonists can in principle be developed through modifying the structure of C5a itself or that of small components of C5a. Site-directed mutagenesis experiments[5–8] on C5a have demonstrated that multiple residues of this 74-amino acid 4-helix bundle protein interact with the receptor. The interhelical loops of C5a (loop 1, $C5a_{13-17}$; loop 3, $C5a_{40-45}$) containing positively charged amino acids are thought to bind to a negatively charged extracellular region of the receptor and together constitute a major ligand–receptor binding domain.[10] The receptor binding "effector" domain of C5a is located at its C-terminus and is entirely responsible for receptor activation leading to signal transduction.[11] Early studies on C5a and fragments of C5a established that the bulk of the molecule away from the C-terminal end contained the receptor recognition site, while the receptor activation domain was localized to the C-terminal region.[9] This ligand–receptor interaction has been recently termed the "two-site" binding hypothesis and may be a general characteristic of G protein-coupled receptors and their endogenous high-molecular-weight ligands.[10]

In an effort to develop C5aR antagonists, several groups have synthesized small-peptide analogues (6–15 amino acids) derived from the C-terminus of C5a which have increased affinities for the C5a receptor and are more potent C5a agonists than the corresponding C-terminal residues of the native C5a sequence.[12–18]

Some small-peptide agonists derived from the C-terminal decapeptide sequence of C5a were found to have partial agonist properties in PMNs[14,19] and have been modified to produce the first complete antagonist, MeFKPdChaWr.[20] On PMN membranes the affinity of this hexapeptide for C5a receptors was only 0.04% that of C5a.[20] Apart from a recent study from our laboratories,[21] there have been no succeeding reports of low-molecular-weight C5a antagonists with increased potency compared to MeFKPdChaWr. Although high-affinity protein C5a antagonists have been recently described by site-directed mutagenesis of C5a,[22,23] such large molecules are expensive to manufacture, have low bioavailabilities and poor pharmacokinetic properties for use as drugs, and would need to be administered parenterally. Indeed, proteins and peptides generally have low bioavailability and poor metabolic stability making them unsuitable as oral drug candidates. To overcome these problems, an orally bioavailable C5a antagonist will need to be a small molecule (MW = 1000 Da) with reduced peptide character and greater potency than MeFKPdChaWr.

* Address correspondence to S. M. Taylor (fax, +61-7-3365-1766; e-mail, s.taylor@mailbox.uq.edu.au).
† Department of Physiology and Pharmacology.
‡ Centre for Drug Design and Development.

Table 1. Structure−Activity Relationships of C5a Antagonist Peptides

no.	peptide	receptor affinity			antagonist potency		
		$-\log IC_{50}$ ($\pm$SE)^a	IC$_{50}$ (μM)^a	n	$-\log IC_{50}$ ($\pm$SE)^b	IC$_{50}$ (μM)^b	n
1	MeFKPdChaW**r**	5.70 ± 0.06	2.0	29	6.97 ±0.09	0.1	17
2	MeFKPdChaW**R**	4.95 ± 0.06*	11	5	5.71 ± 0.35*	2	6
3	**F**KPdChaWr	5.71 ± 0.08	2.0	2	5.17 ± 0.22*	6.8	3
4	**A**KPdChaWr	>3	>1000	2	ND		
5	**Ac**FKPdChaWr	5.32 ± 0.10	4.8	2	ND		
6	**K**FKPdChaWr	5.58 ± 0.26	2.6	3	6.57	0.3	1
7	**FK**FKPdChaWr	5.34 ± 0.08	4.6	3	6.30	0.5	1
8	**C5a**$_{12-20}$-**ahx**-FKPdChaWr	5.91 ± 0.11	1.2	5	6.61 ± 0.12	0.2	4
9	**C5a**$_{12-20}$-**ahx**-**GGGG**-FKPdChaWr	6.76 ±0.08*	0.2	3	7.14 ± 0.16	0.07	4
10	**C5a**$_{40-68}$–FKPdChaWr	5.72 ± 0.04	1.9	3	ND		
11	AcF**O**PdChaWr	6.10 ± 0.26	0.8	3	6.72 ± 0.19	0.2	3
12	AcF**x**PdChaWr^c	5.52 ± 0.14	3.0	3	6.06 ± 0.07*	0.9	3
13	AcF**Nle**PdChaWr	5.45 ± 0.14	3.6	3	5.85 ± 0.38*	1.4	3
14	F**A**PdChaWr	5.04 ± 0.42	9.0	9	5.44 ± 0.11*	3.7	4
15	F**W**PdChaWr	5.23 ± 0.04	5.9	3	6.50 ± 0.17	0.3	3
16a	AcFKPdCha**Z**r^d	4.29 ± 0.10*	51	3	ND		
16b	AcFKPdCha**Z**r^e	3.94 ± 0.10*	116	3	ND		

^{a} $-\log IC_{50}$ and IC$_{50}$, concentration of peptide resulting in 50% inhibition in the binding of [^{125}I]C5a to intact PMNs. ^{b} $-\log IC_{50}$ and IC$_{50}$, concentration of peptide resulting in 50% inhibition of C5a (100 nM) causing the release of MPO from PMNs. ^{c} x, β-aminoalanine or 2,3-diaminopropanoic acid (Dap). ^{d} Z, fluorenylalanine isomer I (see Experimental Section). ^{e} Z, fluorenylalanine isomer II (see Experimental Section); O, ornithine; n, number of experiments performed. Substituted amino acids are highlighted in boldface. *Significant change in affinity/potency compared to MeFKPdChaWr ($p < 0.05$). ND, not determined.

We have recently shown that the hexapeptide C5a antagonist MeFKPdChaWr (**1**) has significant structure in solution,[21] and we now report attempts to stabilize its bioactive turn conformation by specific side chain to backbone cyclizations of the peptide. This approach can increase receptor affinity and antagonist potency while reducing the peptide character of the antagonist. Structure−function relationships are explored for a series of acyclic and cyclic antagonists derived from the C-terminus of C5a which illustrate the merit of structurally preorganizing the antagonist for receptor binding.

1
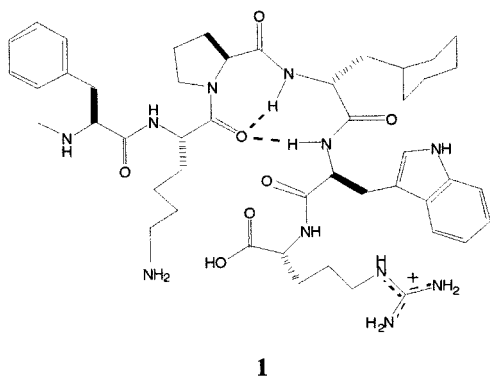
Results and Discussion

Our previous NMR structure study of MeFKPdChaWr (**1**) led us to believe that a turn conformation centered around the K−P−dCha−W residues would engender antagonist activity.[21] That study revealed that while an inverse γ-turn involving K−P−dCha residues persisted in solution, there was only a small conformational population with a larger β-turn involving K−P−dCha−W residues, and the N- and C-termini were quite flexible. We considered that cyclization might stabilize such a turn conformation, reducing the conformational freedom of the N- and C-termini thereby increasing antagonist potency, but needed to first discover which residues in **1** could be modified without losing antagonist potency.

Peptidic Antagonists. Table 1 summarizes the effects of amino acid substitutions in MeFKPdChaWr

(**1**) on receptor affinity and antagonist potency, as measured respectively by competition with [^{125}I]C5a on whole PMNs and inhibition of myeloperoxidase (MPO) release from PMNs induced by a maximal concentration (100 nM) of C5a. The antagonist MeFKPdChaWr (**1**) has N-methyl and D-Arg residues to protect both ends of the molecule from peptide cleavage by endopeptidases in serum, but the effects of other substitutions at the N- and C-termini were not known and were investigated first.

Substitution at the C-terminus of L-Arg for D-Arg (**2** vs **1**) led to a 5−20-fold decrease in both receptor affinity and antagonist potency (Figure 1). We therefore retained D-Arg (designated r) at the C-terminus in all other peptides shown in Table 1. At the N-terminus, the phenylalanine is necessary for both receptor binding and antagonism since replacement by alanine dramatically reduces activity to undetectable levels (**4** vs **3**). Neither methylation nor acetylation of this N-terminal phenylalanine significantly affects receptor affinity (**1** and **5** vs **3**), suggesting the possibility of chain extension to increase activity.

Extension of the hexapeptide at its N-terminus by one or two additional residues (**6, 7**), Lys and Phe being chosen because of their reported importance in longer agonist peptides,[18] failed to increase affinity for the receptor. Addition of a longer peptide sequence, corresponding to one of the interhelical loops (C5a$_{12-20}$, KYKHSVVKK, loop 1) of the 4-helix bundle of C5a, to the N-terminus of the peptide agonist YSFKPMPLaR has been shown to increase receptor binding affinity and activation of the C5a receptors on human PMNs.[18] To investigate if the binding affinity and biological potency of the antagonist could be similarly enhanced, loop 1 (C5a$_{12-20}$) was connected to the N-terminus of FKPdChaWr via an ϵ-aminohexanoic acid linker (**8**), and peptide **9** has an additional four glycines in the linker to further increase the separation between the two motifs. This longer spacer led to significantly increased receptor binding for **9**, but this was not accompanied by an increase in antagonist potency (Table 1). Addition
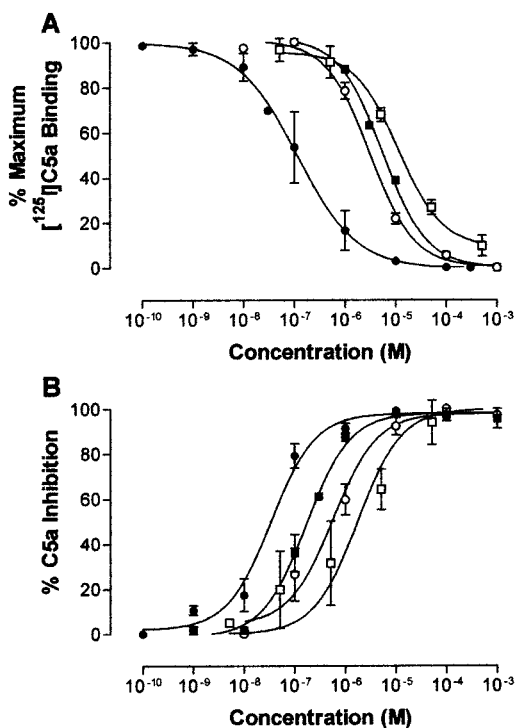
Figure 1. Effects of L-Arg and D-Arg on receptor affinity and antagonist potency: differences between linear and cyclic C5a antagonists. Panel A: Receptor binding as percent inhibition of binding of [^{125}I]C5a to human PMNs. Panel B: C5a antagonist potency as inhibition of MPO release from human PMNs: MeFKPdChaWr, **1** (■); MeFKPdChaWR, **2** (□); F[OPdChaWR], **22** (●); and F[OPdChaWr], **21** (○). Data are means ± SEM.

of a different sequence corresponding to interhelical loop 3 of C5a (C5a$_{37-46}$, RAARISLGPR) did not increase receptor affinity of MeFKPdChaWr (**10**; Table 1), as noted for modified agonist peptides.[18]

Returning to the hexapeptide **1**, substitution of lysine by ornithine (**11**), β-aminoalanine (**12**), norleucine (**13**), alanine (**14**), or tryptophan (**15**) had a relatively small effect on receptor binding (Table 1). Since the side chain length, charge, and hydrophobicity at this position have only a small effect on affinity for the C5a receptor, we considered this site to be promising for linking to the C-terminus of the antagonist to form cyclic analogues (see ahead).

The role of proline has been previously investigated for the C-terminal decapeptide agonist YSFKDMQLGR, in which a proline scan showed optimum affinity for YSFKDM**P**LaR.[18] Since proline is in a corresponding position in the turn-containing antagonist **1**, and because proline plays a unique role in restricting conformational flexibility in peptides due to its restricted ϕ, ψ angles, we did not attempt to substitute it with other amino acids that could compromise the constraint at this position.

Similarly, the role of hydrophobic residues has previously been investigated in the agonist octapeptide AcHKD**ChaCha**LaR and in the antagonists MeFKP**d-Cha**Wr and MeFKPLWr, in which dCha confers at least a 10-fold increase in receptor affinity.[12,13,20] Since cyclohexylalanine is one of the larger hydrophobic amino acids, we did not attempt to further increase steric bulk or hydrophobicity at this position.

The tryptophan of **1** has previously been reported to be important for antagonist activity,[20] but we wondered whether other bulky substituents might be tolerated at this position. In particular we were interested in incorporating fluorescent substituents as labels to permit monitoring of ligand–receptor interactions. A fluorenylalanine side chain (**16**) significantly decreased affinity for the receptor, consistent with the previously observed requirement for a side chain of specific bulk (e.g., Trp) at this position to confer antagonism.[20] Clearly, while Phe and Leu are smaller than required to cause antagonism,[20] the fluorenylalanine is sterically too bulky and agonism was observed instead (EC$_{50}$ = 1 μM, **16a**; 8 μM, **16b**). We conclude that for complete antagonism the hydrophobic space accommodating this substituent must be optimally occupied and that smaller or larger substituents than the indole ring of tryptophan may lead to agonist activity.

Indole group   Fluorenyl group
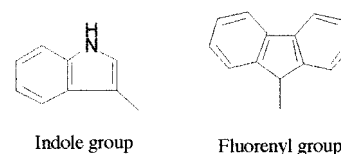
Cyclic Antagonists. Next we aimed to limit the conformational flexibility of the peptide MeFKPdChaWr (**1**) by producing cyclic derivatives which could potentially stabilize a turn motif. The peptide can in principle be cyclized through backbone-to-backbone connection of N- and C-termini (e.g., A) or through various backbone-to-side chain connections (e.g., B). The effects of cyclization on receptor affinity and antagonist potency are summarized in Table 2 for some molecules representing examples A and B.
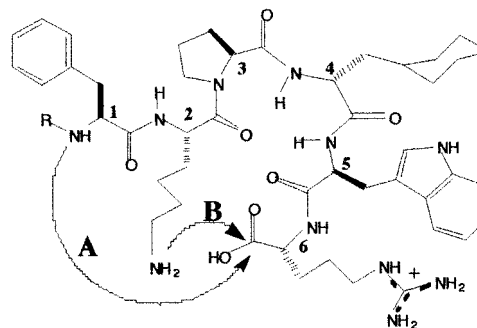
The simplest approach to cyclize the peptide is to covalently link the N- and C-termini through backbone-to-backbone cyclization (A). Thus [FWPdChaWr] (**17**) and its methylated derivative Me[FWPdChaWr] (**18**) were synthesized and assayed (Table 2). For synthetic convenience these cycles contained Trp in place of the Lys of **1** to enable the use of an unprotected peptide in the cyclization reaction, this replacement being shown to maintain affinity in peptide **15** (Table 1). Cycle **18** (Figure 4) had an equivalent affinity to that of the acyclic **1** for the PMN C5a receptor, whereas the nonmethylated cycle **17** had considerably reduced affinity. Thus, peptide **1** may be cyclized without apparent loss of affinity for the receptor, but backbone-to-backbone cyclization did not increase receptor affinity or antagonist potency.

Table 2. Structure−Activity Relationships of Cyclic C5a Antagonists

		receptor affinity			antagonist potency		
no.	peptide	$-\log IC_{50} \pm SE^a$	IC_{50} $(\mu M)^a$	n	$-\log IC_{50} \pm SE^b$	IC_{50} $(\mu M)^b$	n
17	[FWPdChaWr]	4.37 ± 0.36*	43	3	ND		
18	Me[FWPdChaWr]	5.53 ± 0.11	3.0	3	5.82 ± 0.18*	2.1	3
19	F[**K**PdChaWr]	5.09 ± 0.08	8.1	3	5.55 ± 0.57*	2.8	3
20	F[**K**PdChaW**R**]	6.48 ± 0.16*	0.3	3	6.69 ± 0.04	0.2	3
21	F[**O**PdChaWr]	5.51 ±0.07	3.1	3	5.79 ± 0.34*	1.6	3
22	F[**O**PdChaW**R**]	7.25 ± 0.03*	0.06	3	7.46 ±0.09*	0.03	6
23	F[**Dab**PdChaWr]	5.42 ± 0.05	3.8	3	6.70 ± 0.04	0.2	3
24	F[**Dab**PdChaW**R**]	6.51 ± 0.02*	0.3	5	7.36 ± 0.13	0.04	3
25	F[**Dap**PdChaWr]	4.39 ± 0.10*	41	3	ND		
26	F[**Dap**PdChaW**R**]	4.98 ± 0.05*	10	3	5.63 ± 0.13*	2.4	3
27	AcF[**O**PdChaW**R**]	6.57 ± 0.05*	0.3	3	7.69 ±0.13*	0.02	6
28	AcF[**K**PdChaWr]	5.49 ± 0.22	3.2	4	7.07 ± 0.29	0.1	5
29	AcF[**O**PdChaWr]	4.60 ± 0.06*	16	4	6.41 ± 0.10	0.4	4
30	AcF[**Dab**PdChaWr]	4.77 ± 0.14*	17	3	6.09 ± 0.08*	0.8	4
31	AcF[**Dap**PdChaWr]	5.02 ± 0.07	9.5	3	4.71 ± 0.23*	20	3

^{a} $-\log IC_{50}$ and IC_{50}, concentration of peptide resulting in 50% inhibition in the binding of $[^{125}I]C5a$ to intact PMNs. ^{b} $-\log IC_{50}$ and IC_{50}, concentration of peptide resulting in 50% inhibition of C5a (100 nM) causing the release of MPO from PMNs. [ ], cyclization between the ends of the bracketed residues; Dap, L-2,3-diaminopropanoic acid; Dab, L-2,4-diaminobutanoic acid; O, L-ornithine; n, number of experiments performed. Substituted amino acids are highlighted in boldface. *Significant change in affinity/potency compared to MeFKPdChaWr ($p < 0.05$). ND, not determined.
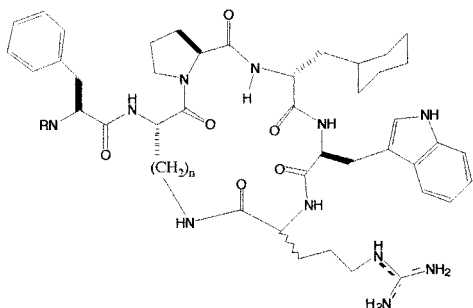
19-31

On the other hand, backbone-to-side chain cyclization (B), specifically by connecting the C-terminal carboxylate to the lysine side chain which had not affected receptor binding (Table 1), was more promising. The resulting cycle **19** ($n = 4$; R = H; D-Arg) did not affect affinity for the C5a receptor on human PMNs versus **1**, but its diastereomer **20** ($n = 4$; R = H, L-Arg) had almost an order of magnitude higher affinity than **1**. This arginine residue is directly involved in cyclization so its chirality could be expected to influence the conformation of the cycle. By varying the length of the linker in **19** ($n = 1−4$), the size of the cycle could also be easily altered, and because of the activity difference between **19** and **20**, we compared the activities for each pair of arginine isomers for each size cycle.

Compounds **19** and **20** were thus compared with analogues in which lysine was replaced with progressively smaller amines such L-ornithine (Orn, $n = 3$; **21**, **22**), L-2,4-diaminobutanoic acid (Dab, $n = 2$; **23**, **24**), and L-2,3-diaminopropanoic acid (Dap, $n = 1$; **25**, **26**). In each case the antagonist activity was greatest when the cycles contained L-arginine instead of D-arginine (Table 2, Figure 1), which is the opposite trend to that observed for the acyclic compounds (Table 1). The larger cycles with Lys, Orn, and Dab were also more potent compounds in terms of both receptor affinity and antagonist potency. Compared to the smaller cycles containing Dap (**25**, **26**) which had 5−20-fold reduced affinity versus **1**, cycles containing L-arginine and ornithine (**22**) or Dab (**24**) bound the receptor with 7−30-fold higher affinity than **1** and displayed antagonist potencies of about 30−
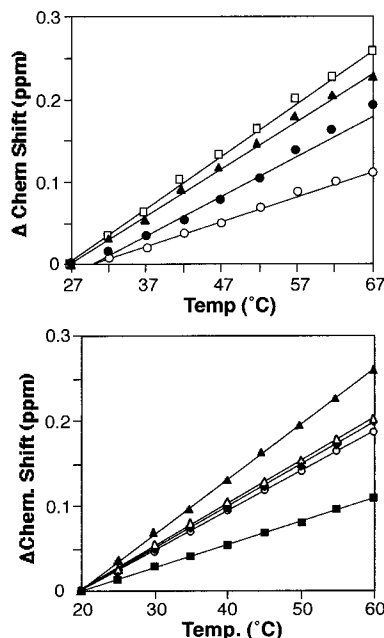
Figure 2. Temperature dependence (20−70 °C) of chemical shifts for amide NH protons of **18** (top) and **27** (bottom) in DMSO-d_6: D-Arg6, □; L-Arg6, ■; Trp5, ▲; dCha4, ○; Orn2, △; Phe1, ◆; Trp2, ●.

40 nM (Table 2). Thus, the size of the cycle had a significant effect on the binding affinity of these antagonists with $n = 2$ or 3 preferred, corresponding to macrocycles with 17 or 18 ring atoms. The acetylated analogue of **22** (namely **27**) was even more potent with antagonist activity $IC_{50} = 20$ nM (Table 2). This is the most active compound reported to date as a C5a antagonist.

In our initial study on C5a antagonists,[21] we reported the activity of one of the cyclic compounds tested as a mixture of Arg diastereoisomers, AcF[OPdChaWr] (**29**) and AcF[OPdChaWR] (**27**). Since the D-Arg conferred higher affinity and antagonist potency in the corresponding linear peptides, we stereoselectively synthesized **29** and determined its NMR solution structure in that study. We have now isolated and tested both diastereomers and find that, contrary to the results for the
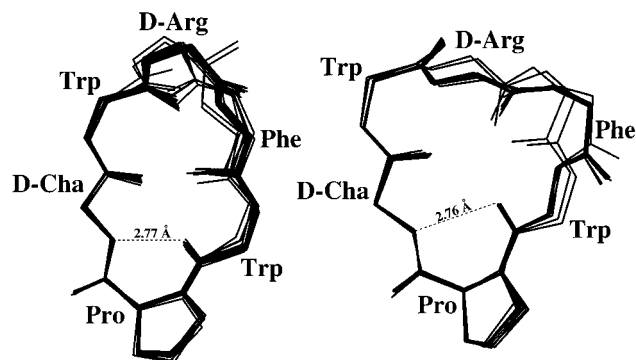
Figure 3. Backbone and proline heavy atoms of 29 low-energy-minimized NMR structures of backbone cycle **18** in DMSO-d_6 (24 °C). Two sets of conformations **18a** (left, 18 structures) and **18b** (right, 11 structures) are shown along with the putative H-bond length (dotted lines) for Trp C**O**···H**N** dCha (**18a**, 2.77 Å; **18b**, 2.76 Å).

Table 3. ^{1}H NMR Assignments[a] for **18** in DMSO-d_6

residue	HN	Hα	Hβ	Hγ	others
MePhe1		3.79	2.92		1.82[b]
Trp2	8.80	4.93	2.87, 3.10		NH 10.80, 7.10[c]
Pro3		4.25	2.02, 1.89	1.74	3.42, 3.69[d]
dCha4	7.82	4.30	1.28		0.74, 1.22
Trp5	8.07	4.58	2.97, 3.10		NH 10.80, 7.10[b]
D-Arg6	8.48	4.46[e]	1.67, 1.89[e]	1.92	3.62[d]
		4.57[f]	1.80, 2.02[f]		

[a] Referenced to residual DMSO-d_5 at 2.50 ppm. [b] N-Me. [c] Aromatics. [d] Hδ. [e] Isomer I. [f] Isomer II.
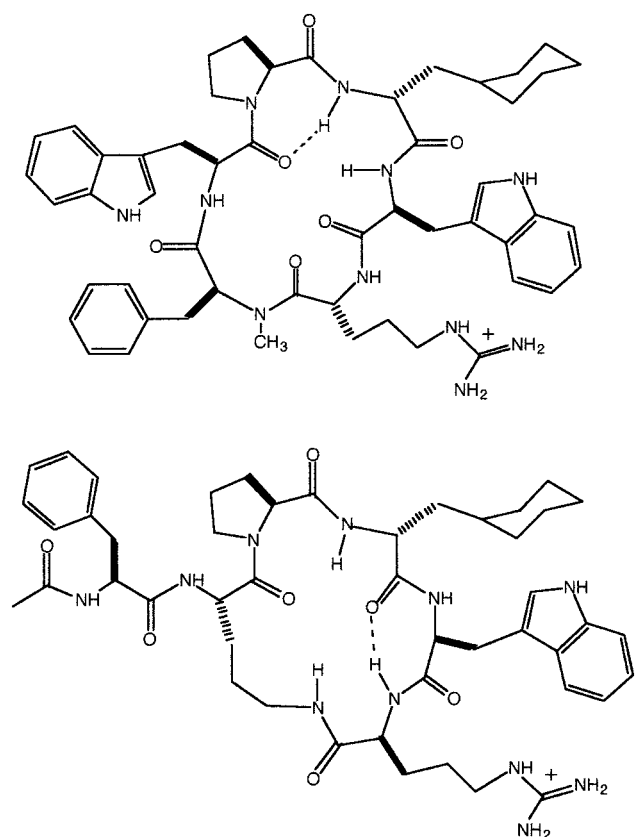
Figure 4. Structures of cycles **18** (top) and **27** (bottom) showing components and connectivity.

linear peptide diastereomers, **27** with L-Arg is actually much more active than **29** which contains D-Arg. Figure 1 summarizes this activity difference. Panel A compares the receptor binding of L- and D-Arg isomers for a linear and a cyclic antagonist, while panel B shows the importance of L- versus D-arginine for antagonist potency. For this reason we report in this study the solution structure of the active diastereoisomer **27** for comparison with the previously determined structure of the less active antagonist **29**.

In our earlier preliminary study on C5a antagonists, we reported that there was a good correlation between binding affinity and antagonist potency.[21] Although increases in affinity for the PMN C5a receptor were usually accompanied by increased antagonist potency,

there were some exceptions, notably compounds **9** and **20** (Tables 1 and 2). The reasons for this are not yet clear, but such results reinforce the notion that measurements of both affinity and antagonist potency should be carried out to fully characterize the in vitro activity of new antagonists.

Receptor Selectivity. To determine the selectivity of the cyclic antagonists for the C5aR, compounds **22** and **27** were tested for their ability to block PMN enzyme secretion to other G protein ligands, such as formylmethionyl-leucyl-phenylalanine (fMLP), leukotriene B$_4$ (LTB$_4$), and platelet-activating factor (PAF). Maximally effective agonist concentrations of fMLP (1 μM), LTB$_4$ (0.1 μM), or PAF (1 μM) were used to cause PMN MPO secretion. In concentrations up to 100 μM, neither **22** nor **27** affected fMLP MPO release, and **22** at 100 μM did not affect either LTB$_4$ or PAF MPO release. Some inhibition ($\sim$50%) of PAF and LTB$_4$ MPO secretion was seen with 100 μM **27**. Since both C5a antagonists at concentrations below 1 μM completely inhibited MPO secretion to a maximally effective concentration of C5a (100 nM), the results demonstrate the highly selective nature of the inhibition for the C5aR.

NMR Solution Structure of Cycle 18. An NMR investigation of the solution structure of cycle **18** was carried out to determine the conformational preference for the backbone of this cycle. DQF-COSY and TOCSY two-dimensional NMR spectra were used to identify residue types from their side chain connectivities. NOESY spectra were then used to obtain sequential assignments and chemical shifts listed in Table 3.

H/D exchange and temperature dependence studies were carried out to provide information about intramolecular hydrogen bonds. The 1D ^{1}H NMR spectrum of peptide **18** in DMSO-d_6 at 25 °C shows four distinct resonances in the amide region. A 10-fold excess of D$_2$O was added to this solution to promote exchange of amide NH's with deuterium, and 1D spectra were recorded at regular intervals. Due to fast H/D exchange, the amide NH of Trp2 disappeared rapidly compared to the other three amide NH protons for D-Arg, Trp5, and dCha which remained after 120 min. These peaks persisted for at least another hour after addition of a further 10-fold amount of D$_2$O. This behavior is characteristic of protection from solvent and suggests the possibility of intramolecular hydrogen bonding.

The temperature dependence (27−67 °C) of amide NH chemical shifts for cycle **18** is shown in Figure 2. The temperature coefficients ($\Delta\delta$/T) were 3.0 ppb/deg (dCha NH); 4.8 ppb/deg (Trp2 NH); 5.8 ppb/deg (Trp5 NH); 6.4 ppb/deg (D-Arg NH). Values of $\Delta\delta$/T $\sim$ 3 ppb/deg or less usually indicate solvent protection,[23] so the amide NH of dCha is likely hydrogen-bonded in a majority of

Table 4. Backbone ϕ, ψ Angles (deg) for Peptides **18** and **27**

| residue | ϕ, ψ | | residue | ϕ, ψ |
	18a	**18b**		**27**
Phe1	70, −176	51, −74	Phe1	−167, 56
Trp2	65, −174	−96, 178	Orn2	−97, 146
Pro3	−75, 43	−68, 78	Pro3	−71, 160
dCha4	132, 162	131, 157	dCha4	65, 176
Trp5	55, 86	42, 40	Trp5	−91, 28
D-Arg6	53, 90	60, −173	Arg6	−151, 53

Table 5. ^{1}H NMR Assignments[a] for **27** in DMSO-d_6

residue	HN[b]	Hα	Hβ	Hγ	others
AcPhe	8.10	4.51	2.69, 2.96		1.74 (Me), 7.22[c]
Orn	7.95	4.55	1.44, 1.64	1.22	2.76, 3.38,[d] 7.04 (NHε)
Pro		4.57	1.63, 1.99	1.63	3.41, 3.62[d]
dCha	8.16	4.01	1.15, 1.26	0.93	0.62, 0.69
Trp	8.40	4.28	2.96, 3.26		7.15, 7.39,[c] 10.86 (NH)
Arg	7.81	4.11	1.63, 1.87	1.50	3.11,[d] 7.57 (NHε)

[a] Referenced to residual DMSO-d_5 at 2.50 ppm. [b] Amide NH's, $^3J_{NH-C\alpha H}$ (Hz): 8.51 (Phe), 7.14 (Orn), 4.94 (dCha), 7.14 (Trp), 8.23 (Arg). [c] Aromatic CHs. [d] Hδ.

conformers. On the other hand, the slow exchange behavior but high temperature coefficient of the D-Arg and Trp5 amide NH's reflects solvent protection/intramolecular hydrogen bonding in a much smaller population of solution conformers.

NOESY experiments afforded spectra with a good signal-to-noise ratio, and several of the identified NOEs for this cycle indicated the presence of a folded conformer.[25] These include *i, i*+2 NOEs from Trp2 to dCha and a dCha to Trp5 NH−NH NOE, which suggest a turn in the peptide centered on the Pro−dCha residues. Other significant NOEs were observed between Trp2 αH and the two Pro δH protons. These confirm that the Trp−Pro bond exists in the trans conformation. The presence of *cis*-Pro bonds is not uncommon in small peptides, but in this case there is no evidence of any minor populations containing a cis form of the Trp−Pro bond. However, doubling of signals from residues near the Phe suggested the presence of both cis and trans isomers of the methyl amide bond between Phe and D-Arg, with the trans form predominant.

NOEs detected for the trans isomer of **18** supported the existence of a well-defined conformer and were used to derive a set of 41 interproton distance restraints. These restraints were used to generate a set of 50 structures using a simulated annealing algorithm within the program XPLOR. All of these structures showed a good convergence to a folded conformation; however there are two distinct conformational populations as shown in Figure 3. In the first family of 18 structures a pairwise rmsd of 0.30 Å was obtained for all of the backbone Cα, N, C atoms, while for the second family consisting of 11 structures there was a pairwise rmsd of 0.25 Å. Thus, there was a good superimposition within each family of structures.

The ϕ, ψ angles for the average structure generated from the members of each of the families **18a** and **18b** are given in Table 4. These data reveal that the main differences between the two families reside in MePhe, Trp2, and D-Arg, whereas the region Pro to Trp5 is conserved between the two families. Analysis of the structures revealed the formation of a hydrogen bond between the C=O of Trp2 and NH of dCha to form a 7-membered ring associated with an inverse γ-turn. This is consistent with hydrogen bond formation involving the dCha NH as indicated by the temperature coefficient data. The ϕ, ψ angles for Pro in both families are also consistent with the presence of an inverse γ-turn,[25] and a schematic drawing of the cycle **18** is shown in Figure 4. The hydrogen bond associated with the proposed inverse γ-turn is defined by the dashed line. The inverse γ-turn identified in both structural families of the cycle **18** had a dCha−NH⋯OC−Trp heavy atom distance of 2.77 and 2.76 Å and a N−H⋯O angle of 150° and 135° for families **18a** and **18b**,

respectively. Hence as found for linear peptide **1**,[20] an inverse γ-turn is the major feature of the solution structure of cycle **18**. Potential hydrogen bonding between Trp2 C=O and Trp5 N−H to form a 10-membered ring β-turn was eliminated as a possibility, at least for a majority population of conformers, because of the large distance between the donor and acceptor atoms.

NMR Solution Structure of Cycle 27. ^{1}H NMR spectral data for cycle **27** (Table 5) in DMSO-d_6 at 24 °C shows six distinct amide resonances which are attributed to the amide NH's of residues Phe, Orn, dCha, Trp, and Arg and the side chain of Orn which is linked to the C-terminus. The $^3J_{NH-\alpha H}$ coupling constants for the amide NH protons of cycle **27** were measured from the 1D spectrum and are reported in Table 5. It is unusual for backbone coupling constants in small peptides to differ from the conformationally averaged value of ~7 Hz;[25] therefore, it is significant that the constants are higher for Phe (8.51 Hz) and D-Arg (8.23 Hz) but lower for dCha (4.94 Hz) than the conformational average. These coupling constants strongly indicate the presence of well-defined local structure near these residues in a significant proportion of the solution conformations.

A temperature dependence (20−60 °C) study of the amide NH chemical shifts was also carried out for peptide **27**, and the results are shown graphically in Figure 2. Only one of the NH protons has chemical shift/temperature coefficients ($\Delta\delta$/T) < 3 ppb/deg, and this is assigned to the Arg (2.72 ppb/deg). This low temperature coefficient is highly significant for such a small peptide, indicating intramolecular hydrogen bond formation.

The NOE data are consistent with the cyclic **27** adopting a well-defined solution conformation. In combination with the coupling constant data, several highly characteristic medium range NOEs confirm the presence of an inverse γ-turn involving the residues dCha−Trp−DArg. In particular, the presence of small and large coupling constants for the two residues dCha and Arg, respectively, together with an αH−NHε NOE between Trp5 and Orn, an αH−NH *i, i*+2 NOE between dCha and Arg, and an NH−NH NOE between Trp5 and Arg suggest an inverse γ-turn conformation. This agrees well with the observed low temperature coefficient for the Arg NH proton. From a set of 66 NOE-based distance restraints and 3 dihedral angle (ϕ) constraints, a family of 50 structures was calculated. The structures converged with high precision, and the 20 lowest-energy structures are shown in Figure 5. The rmsd over all backbone atoms of the cycle is 0.35 Å reflecting good superposition of the structures.

The ϕ, ψ angles for the average structure generated from members of family **27** is given in Table 4. The
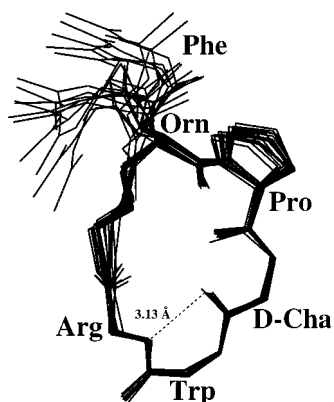
Figure 5. Backbone and proline heavy atoms of 20 lowest-energy-minimized NMR structures of **27** in DMSO-d_6 (24 °C). Putative H-bond length (dotted line) for dCha C**O**⋅⋅⋅H**N** Arg is 3.13 Å.

temperature-dependence study of amide resonances implicated the Arg NH in hydrogen bonding. Analysis of potential hydrogen bonding in the converged structures revealed an inverse γ-turn between the Arg NH and dCha C=O as the most reasonable donor and acceptor residues for hydrogen bonding (H-bond shown in Figure 5). For the inverse γ-turn hydrogen bond in this family an Arg NH⋅⋅⋅O=C dCha heavy atom distance of 3.13 Å and N−H⋅⋅⋅O angle of 140° were found, these values being consistent with inverse γ-turn hydrogen bonds in proteins.[26]

The solution structure of cycle **27** differs somewhat from that determined for either its diastereomer AcF-[OPdChaWr] or the linear peptide **1**[21] and also from the backbone cycle **18** (Figure 3) in that the inverse γ-turn is now situated between residues dCha and Arg, instead of between residues Orn and dCha. This new position for the inverse γ-turn in **27** still enforces a similar overall (turn) conformation upon the cyclic backbone as in **29** or **1** but may orient the side chains differently. Such subtle repositioning of the side chains accounts for the different (increased) binding affinity and antagonist potency for this cycle. While ultimately it would be valuable to directly determine the receptor-bound conformation to confirm this suggestion, we are currently limited to an examination of solution conformations and to the assumption that the cyclic nature of the peptides means that receptor-bound conformations will be similar to that determined in DMSO. The poor solubility of **27** in water precluded a determination of its structure in aqueous solution; however in an attempt to assess possible contributions to side chain conformations from hydrophobic collapse in aqueous solution, we measured chemical shifts and main-chain coupling constants of **27** in a range of DMSO/water mixtures and found that the backbone αH shifts of Orn, dCha, Arg, and Phe varied by less than 0.1 ppm for DMSO/water ratios from 100/0% to 15/85%, and the coupling constants for all backbone residues varied by less than 10% over the same range of solvent mixtures. This strongly suggests that the backbone conformation (and by implication the side chain orientations) do not vary significantly with the solution environment. It can thus reasonably be assumed the receptor-bound conformation is similar to that determined above. In the DMSO/water titrations there was a monotonic shift of the αH peak

of the Trp residue from 4.28 to 4.70 ppm with increasing water concentration. Given the invariance of the other shifts and coupling constants, this most likely reflects minor orientation changes of the Trp side chain (expected to have a large effect on the Trp αH shift due to ring-current effects) rather than a change in the global backbone conformation.

Summary

We have determined structure−activity relationships for a series of cyclic and acyclic analogues of the peptide MeFKPdChaWr, an antagonist of the C5a receptor on human PMNs. Except for the fluorenylalanine derivatives, none of the peptides tested showed any agonist activity in causing the release of MPO from human PMNs in the concentration range of $10^{-10}-10^{-3}$ M. Structure−activity data and NMR solution structures indicate that a general turn conformation is a key structural determinant of antagonist activity in the peptides, a point demonstrated by the improved receptor affinity and antagonist potency of cyclic analogues. Such cycles stabilize a turn conformation, and those with a ring size of 17 or 18 atoms were the most potent compounds, with AcF[OPdChaWR] showing the best C5a antagonist activity (IC_{50} = 20 nM) for human PMNs. Our results provide significant progress toward the development of a pharmacophoric model for small C5a antagonists derived from the C-terminus of C5a and may catalyze the development of a new drug candidate for the treatment of inflammatory diseases. As a step toward this goal, we have recently found that one of these potent cyclic C5a antagonists, F[OPdChaWR], is an effective inhibitor of C5a- and endotoxin- induced neutropenia when administered intravenously to rats.[27]

Experimental Section

Abbreviations: TFA, trifluoroacetic acid; DIEA, diisopropylethylamine; HBTU, *O*-benzotriazole *N,N,N,N*-tetramethyluronium hexafluorophosphate; BOP, benzotriazol-1-yloxytris(dimethylamino)phosphonium hexafluorophosphate; DMF, dimethylformamide; O, L-ornithine; dCha, D-cyclohexylalanine; amino acid symbols "r" and "a" represent D-Arg and D-Ala, respectively; t_R, retention time; ES-MS, electrospray mass spectrometry.

General Methods. Protected amino acids and resins were obtained from Novabiochem. TFA, DIEA, and DMF (peptide synthesis grade) were purchased from Auspep. All other materials were reagent grade unless otherwise stated. Preparative scale reverse-phase HPLC separations were performed on a Vydac C18 reverse-phase column (2.2 × 25 cm); analytical reverse-phase HPLC on Waters Delta-Pak PrepPak C18 reverse-phase column (0.8 × 10 cm); using gradient mixtures of solvent A = water/0.1% TFA and solvent B = water 10%/acetonitrile 90%/0.09% TFA. The molecular weight of the peptides was determined by electrospray mass spectrometry recorded on a triple quadrupole mass spectrometer (PE SCIEX API III) as described elsewhere.[28] ^{1}H NMR spectra were recorded on a Bruker 500 or 750 NMR spectrometer at 24 °C. Proton assignments were determined by 2D NMR experiments (DFCOSY, TOCSY, NOESY). All assay data were analyzed by nonlinear regression and statistics using one-way ANOVA followed by a Newman−Keuls multiple comparisons test.

Peptide Synthesis. The linear peptides **1**−**16** were assembled by manual stepwise solid-phase peptide synthesis using HBTU activation and DIPEA in situ neutralization. Couplings were monitored by the quantitative ninhydrin test. Boc chemistry was employed for temporary N$^\alpha$-protection of amino acids with two 1-min treatments with TFA for Boc group removal. Peptides were synthesized on a Novabiochem

Table 6. Peptide Retention Times (t_R) and Mass Spectral Data[a]

peptide	sequence	t_R (min)	MH+ exptl	MH+ calcd
1	MeFKPdChaWr	32.0	900.5	900.7
2	MeFKPdChaWR	33.4	900.7	900.7
3	FKPdChaWr	33.5	886.7	886.5
4	AKPdChaWr	28.8	810.5	810.6
5	AcFKPdChaWr	31.8	928.5	928.7
6	KFKPdChaWr	28.7	1014.6	1015.0
7	FKFKPdChaWr	30.5	1161.7	1162.0
8	C5a$_{12-20}$-ahx-FKPdChaWr	34.4	2097.3	2097.6
9	C5a$_{12-20}$-ahx-GGGGFKPdChaWr	28.8	2325.4	2326.2
10	C5a$_{40-68}$-FKPdChaWr	31.7	4206.1	4205.1
11	AcFOPdChaWr	38.4	914.5	914.7
12	AcF(Dap)PdChaWr	39.8	886.5	886.7
13	AcFNlePdChaWr	36.2	913.5	913.1
14	FAPdChaWr	33.2	829.5	829.7
15	FWPdChaWr	35.4	944.5	944.7
16a	AcFKPdChaZr (I)	44.7	977.5	977.7
16b	AcFKPdChaZr (II)	47.2	977.5	977.7

[a] Dap, L-2,3-diaminopropanoic acid; Z, fluorenylalanine which was synthesized as a mixture of enantiomers and was introduced into the peptide during peptide synthesis as a mixture. The two peptide diastereomers were subsequently separated using rp-HPLC and are arbitrarily denoted as isomers I and II.

Table 7. Characterization Data (rp-HPLC Retention Times and ES-MS) for Cyclic Peptides[a]

peptide	sequence	t_R (min)	MH+ exptl	MH+ calcd
17	[FWPdChaWr]	41.6	926.5	926.5
18	Me[FWPdChaWr]	42.2	940.5	940.5
19	F[KPdChaWr]	35.3	868.5	868.5
20	F[KPdChaWR]	33.6	868.5	868.5
21	F[OPdChaWr]	36.1	854.5	854.5
22	F[OPdChaWR]	33.8	854.5	854.5
23	F[DabPdChaWr]	32.6	840.5	840.5
24	F[DabPdChaWR]	33.6	840.5	840.5
25	F[DapPdChaWr]	35.4	826.5	826.5
26	F[DapPdChaWR]	32.9	826.5	826.5
27	AcF[OPdChaWR]	39.8	896.5	896.5
28	AcF[KPdChaWr]	44.0	910.5	910.5
29	AcF[OPdChaWr]	43.7	896.5	896.5
30	AcF[DabPdChaWr]	42.0	882.5	882.5
31	AcF[DapPdChaWr]	41.2	868.5	868.5

[a] Dap, L-2,3-diaminopropionic acid; Dab, L-2,4-diaminobutanoic acid; O, L-ornithine; [], cyclization between the ends of the bracketed residues.

Boc-D-Arg(Tos)-PAM or Boc-L-Arg(Tos)-PAM resin with a substitution value of approximately 0.5 mmol/g. The peptides were fully deprotected and cleaved by treatment with liquid HF (10 mL), *p*-cresol (1 mL) at −5 °C for 1−2 h. Analytical HPLC was used for peptide purification (gradient 0 to 75% B over 60 min). Peptide retention times (t_R) and mass spectral data are listed in Table 6.

Peptide Cyclization. The general procedure for cyclization of linear peptides involved dissolving the peptide (1 equiv) and BOP (5 equiv) in DMF (10 mM peptide concentration) and stirring vigorously, followed by the addition of DIEA (15 equiv). Solutions were generally allowed to stir at room temperature overnight, although in most cases the reaction was complete within 2 h. DMF was removed under high vacuum at 30 °C on a rotary evaporator and then purified by rp-HPLC. For cyclic peptides containing a free N-terminus, a Fmoc group was used as the temporary N-terminal protecting group during the cyclization step. DMF was removed under high vacuum at 30 °C on a rotary evaporator, and then the peptide was treated with 30% piperidine/DMF for 1 h at room temperature to remove the Fmoc group. This was followed by solvent removal under high vacuum and purification by rp-HPLC. Representative examples of the various methods of synthesis of the cycles follows.

Synthesis of Cycle Me[FWPdChaWr] (18). The linear peptide MeF-W-P-dCha-W-r was synthesized by Boc chemistry on a 0.1-mmol scale using HBTU/DIEA activation and in situ neutralization on a Boc-D-Arg(Tos)-PAM resin (169 mg, SV = 0.77 mmol/g). Cleavage and deprotection of the resin (97 mg) were achieved by treating the resin with HF (10 mL) and *p*-cresol (1 mL) at −5 to 0 °C for 1−2 h, and the crude peptide was purified by rp-HPLC (13.7 mg, 38%). Cyclization involved stirring the crude peptide (7.25 mg, 7.6 μmol), BOP (12 mg, 26.6 μmol), and DIEA (13 μL, 0.08 mmol) in DMF (18 mL) for 15 h. The solvent was removed in vacuo and the cyclic peptide purified by rp-HPLC (1.92 mg, 27%): t_R = 42.2 min; MS [M + H]+ calcd = 940.5, [M + H]+ exptl = 940.7.

Synthesis of Cycle F[KPdChaWR] (20). The linear peptide Fmoc-Phe-Lys-Pro-dCha-Trp-Arg was synthesized by Boc chemistry on a 0.05-mmol scale using HBTU/DIEA activation on a Boc-L-Arg(Tos)-PAM resin (114 mg, SV = 0.44 mmol/g). Cleavage and deprotection of the resin (93 mg) were achieved by treating with HF (10 mL) and *p*-cresol (1 mL) at −5 to 0 °C for 1−2 h to give the crude peptide (28 mg, 94%). Cyclization involved stirring the crude peptide (28 mg, 25 μmol), BOP (49 mg, 0.11 mmol), and DIEA (38 μL, 0.2 mmol) in DMF (22 mL) for 15 h. The solvent was removed in vacuo

and the Fmoc protecting group removed by treating with 30% piperidine/DMF (4 mL) for 1 h. The solvents were removed in vacuo, and the cyclic peptide was purified by rp-HPLC (4.8 mg, 22%): t_R = 33.6 min; MS [M + H]+ calcd = 868.5, [M + H]+ exptl = 868.5.

Synthesis of Cycle AcF[OPdChaWR] (27). The linear peptide Ac-Phe-Orn-Pro-dCha-Trp-Arg was synthesized by Boc chemistry on a 0.20-mmol scale using HBTU/DIEA activation and in situ neutralization on a Boc-L-Arg(Tos)-PAM resin (338 mg, SV = 0.591 mmol/g). Cleavage and deprotection of the resin (457 mg) were achieved by treating the resin with HF (10 mL) and *p*-cresol (1 mL) at −5 to 0 °C for 1−2 h, to give crude peptide (160 mg, 90%). Cyclization involved stirring the crude peptide (41 mg, 45 μmol), BOP (126 mg, 0.28 mmol), and DIEA (158 μL, 0.9 mmol) in DMF (57 mL) for 15 h. The solvent was removed in vacuo and the cyclic peptide purified by rp-HPLC (18.8 mg, 47%): t_R = 43.7 min; MS [M + H]+ calcd = 896.5, [M + H]+ exptl = 896.5.

Purification and Characterization. Crude peptides were purified using preparative rp-HPLC using a Vydac C18 reverse-phase column (2.2 × 25 cm). Gradients of 1 mL/min of solvent A to solvent B were employed and monitored at 214 nm. Fractions were collected and tested by electrospray mass spectrometry (ES-MS) for the correct molecular weight, and purity was checked by analytical rp-HPLC on a Waters Delta-Pak PrepPak C18 reverse-phase column (0.8 × 10 cm) (gradient 0 to 75% B over 60 min). The acetonitrile was HPLC grade (BDH Laboratories), and TFA was synthesis grade (Auspep). Characterization data (rpHPLC retention times and ES-MS) for cyclic peptides are shown in Table 7.

NMR Structure Determination. ^{1}H NMR spectra were recorded for 3 mg of **18** and **27** in 550 μL DMSO-d_6 and chemical shifts were referenced to the solvent signal. 2D ^{1}H NMR NOESY (relaxation delay 2.0 s, mix time 150−300 ms), DQF-COSY, and TOCSY (mixing time 80 ms) experiments were recorded in phase-sensitive mode. Acquisition time = 0.170 s, spectral width = 12 000 Hz, with F_1 = 4096 and F_2 = 700.

NMR data were processed using UXNMR software (Bruker) on a Silicon Graphics Indy workstation. 2D NOE cross-peaks were characterized into strong (1.8−2.7 Å), medium (1.8−3.5 Å), and weak (1.8−5.0 Å) based on their intensities. Backbone dihedral restraints were inferred from $^3J_{NH-H\alpha}$ coupling constants with ϕ restrained to −120 ± 40° for $^3J_{NH-H\alpha}$ > 8 Hz, −65 ± 25° for J < 5 Hz[29] for L-amino acids, and +120 ± 40° for $^3J_{NH-H\alpha}$ > 8 Hz in dCha. Three-dimensional structures were calculated using a simulated annealing and energy minimization protocol in the program XPLOR 3.1.[30] In the first step an ab initio simulated annealing protocol[31] was used, starting from template structures with randomized ϕ and ψ angles and extended side chains, to generate a set of 50 structures. The

simulated annealing protocol consisted of 20 ps of high-temperature molecular dynamics (1000 K) with a low weighting on the repel force constant and NOE restraints. This was followed for a further 10 ps with an increased force constant on the experimental NOE restraints. The dihedral force constant was increased prior to cooling the system to 300 K and increasing the repel force constant over 15 ps of dynamics. Refinement of these structures was achieved using the conjugate gradient Powell algorithm with 1000 cycles of energy minimization[32] and a refined force field based on the program CHARM.[33] Structures were displayed using INSIGHT (Biosym Technologies, San Diego, CA). All structural analysis described in the text was done using structures calculated without explicit H-bond restraints. The final structures were examined to obtain pairwise rms differences over the backbone heavy atoms (N, Cα, and C).

Receptor Binding Assay. Assays were performed with fresh human PMNs, isolated as previously described,[18] and a buffer of 50 mM HEPES, 1 mM $CaCl_2$, 5 mM $MgCl_2$, 0.5% bovine serum albumin, 0.1% bacitracin, and 100 μM PMSF (phenylmethanesulfonyl fluoride). Buffer, unlabeled human recombinant C5a (Sigma) or test peptide, [^{125}I]C5a ($\sim$50 pM) (New England Nuclear, MA), and PMNs (0.2×10^6) were added sequentially to a Millipore Multiscreen assay plate. After incubation for 60 min at 4 °C, the samples were filtered and the plate was washed once with buffer (100 μL). Filters were dried, punched, and counted in an LKB γ-counter. Nonspecific binding was assessed by the inclusion of 1 mM peptide or 100 nM C5a which typically resulted in 10−15% total binding.

Antagonism Assay. Antagonist assays were assessed by monitoring myeloperoxidase release as follows. Cells were isolated as previously described[18] and incubated with cytochalasin B (10 μg/mL, 10 min, 37 °C). Hank's balanced salt solution containing 0.1% gelatin and test peptide was added onto a 96-well plate (total volume 100 μL/well), followed by 25 μL of cells (4×10^6/mL). To assess the capacity of each peptide to antagonize C5a, cells were incubated for 10 min at 37 °C with each peptide, followed by addition of C5a (100 nM) and further incubated for 10 min. Then 50 μL of phosphate buffer (0.1 M, pH 6.8) was added to each well, followed by the addition of 25 μL of a fresh 1:1 mixture of dimethoxybenzidine (5.7 mg/mL) and H_2O_2 (0.51%). The reaction was stopped at 20 min by addition of 2% sodium azide (25 μL). Absorbances were measured at 450 nm in a Rainbow plate reader and corrected for control values (no peptide).

References

(1) Jose, P. J.; Moss, I. K.; Maini, R. N.; Williams, T. J. Measurement of the chemotactic complement fragment C5a in rheumatoid synovial fluids by radioimmunoassay: role of C5a in the acute inflammatory phase. *Ann. Rheum. Dis.* **1990**, *49*, 747−52.
(2) Valazquez, P.; Cribbs, D. H.; Poulos, T. L.; Tenner, A. J. Aspartate residue 7 in amyloid beta protein is critical for classical complement pathway activation: implications for alzheimers disease pathogenesis. *Nature Med.* **1997** *3*, 77−9.
(3) Engler, R. L.; Roth, D. M.; del Balzo, U.; Ito, B. R. Intracoronary C5a induces myocardial ischemia by mechanisms independent of the neutrophil: leukocyte filters desensitize the myocardium to C5a. *FASEB J.* **1991**, *5*, 2983−91.
(4) Hammerschmidt, D. E.; Weaver, L. J.; Hudson, L. D.; Craddock, P. R.; Jacob, H. S. Association of complement activation and elevated plasma C5a with adult respiratory distress syndrome. Pathophysiological relevance and possible prognostic value. *Lancet* **1980**, *1*, 947−9.
(5) Mollison, K. W.; Mandecki, W.; Zuiderweg, E. R.; Fayer, L.; Fey, T. A.; Krause, R. A.; Conway, R. G.; Miller, L.; Edalji, R. P.; Shallcross, M. A.; et al. Identification of receptor-binding residues in the inflammatory complement protein C5a by site-directed mutagenesis. *Proc. Natl. Acad. Sci. U.S.A.* **1989**, *86*, 292−6.

(6) Bubeck, P.; Grotzinger, J.; Winkler, M.; Kohl, J.; Wollmer, A.; Klos, A.; Bautsch, W. Site-specific mutagenesis of residues in the human C5a anaphylatoxin which are involved in possible interaction with the C5a receptor. *Eur. J. Biochem.* **1994**, *219*, 897−904.
(7) Federwisch, M.; Wollmer, A.; Emde, M.; Stuhmer, T.; Melcher, T.; Klos, A.; Kohl, J.; Bautsch, W. Tryptophan mutants of human C5a anaphylatoxin: a fluorescence anisotropy decay and energy transfer study. *Biophys. Chem.* **1993**, *46*, 237−48.
(8) Toth, M. J.; Huwyler, L.; Boyar, W. C.; Braunwalder, A. F.; Yarwood, D.; Hadala, J.; Haston, W. O.; Sills, M. A.; Seligmann, B.; Galakatos, N. The pharmacophore of the human C5a anaphylatoxin. *Protein Sci.* **1994**, *3*, 1159−68.
(9) Chenoweth, D. E.; Hugli, T. E. Human C5a and C5a analogues as probes of the neutrophil C5a receptor. *Mol. Immunol.* **1980**, *17*, 151−61.
(10) Siciliano, S. J.; Rollins, T. E.; DeMartino, J.; Konteatis, Z.; Malkowitz, L.; VanRiper, G.; Bondy, S.; Rosen, H.; Springer, M. S. Two-site binding of C5a by its receptor: an alternative binding paradigm for G protein-coupled receptors. *Proc. Natl. Acad. Sci. U.S.A.* **1994**, *91*, 1214−8.
(11) DeMartino, J. A.; Van Riper, G.; Siciliano, S. J.; Molineaux, C. J.; Konteatis, Z. D.; Rosen, H.; Springer, M. S. The amino terminus of the human C5a receptor is required for high affinity C5a binding and for receptor activation by C5a but not C5a analogues. *J. Biol. Chem.* **1994**, *269*, 14446−50.
(12) Kawai, M.; Quincy, D. A.; Lane, B.; Mollison, K. W.; Luly, J. R.; Carter, G. W. Identification and synthesis of a receptor binding site of human anaphylatoxin C5a. *J. Med. Chem.* **1991**, *34*, 2068−71.
(13) Kawai, M.; Quincy, D. A.; Lane, B.; Mollison, K. W.; Or, Y.-S.; Luly, J. R.; Carter, G. W. Structure−function studies in a series of carboxyl-terminal octapeptide analogues of anaphylatoxin C5a. *J. Med. Chem.* **1992**, *35*, 220−3.
(14) Mollison, K. W.; Krause, R. A.; Fey, T. A.; Miller, L.; Wiedeman, P. E.; Kawai, M.; Lane, B.; Luly, J. R.; Carter, G. W. Hexapeptide analogues of C5a anaphylatoxin reveal heterogeneous neutrophil agonism/antagonism. *FASEB J.* **1992**, *6*, A2058.
(15) Ember, J. A.; Sanderson, S. D.; Taylor, S. M.; Kawahara, M.; Hugli, T. E. Biologic activity of synthetic analogues of C5a anaphylatoxin. *J. Immunol.* **1992**, *148*, 3165−73.
(16) Sanderson, S. D.; Ember, J. A.; Kirnarsky, L.; Sherman, S. A.; Finch, A. M.; Taylor, S. M. Decapeptide agonists of human C5a: the relationship between conformation and spasmogenic and platelet aggregatory activities. *J. Med. Chem.* **1994**, *37*, 3171−80.
(17) Sanderson, S. D.; Kirnarsky, L.; Sherman, S. A.; Vogen, S. M.; Prakesh, O.; Ember, J. A.; Finch, A. M.; Taylor, S. M. Decapeptide agonists of human C5a: the relationship between conformation and neutrophil response. *J. Med. Chem.* **1995**, *38*, 3669−75.
(18) Finch, A. M.; Vogen, S. M.; Sherman, S. A.; Kirnarsky, L.; Taylor, S. M.; Sanderson, S. D. Biological active conformer of the effector region of human C5a and modulatory effects of N-terminal receptor binding determinants on activity. *J. Med. Chem.* **1997**, *40*, 877−84.
(19) Drapeau, G.; Brochu, S.; Godin, D.; Levesque, L.; Rioux, F.; Marceau, F. Synthetic C5a receptor agonists. Pharmacology, metabolism and in vivo cardiovascular and hematologic effects. *Biochem. Pharmacol.* **1993**, *45*, 1289−99.
(20) Konteatis, Z. D.; Siciliano, S. J.; Van Riper, G.; Molineaux, C. J.; Pandya, S.; Fischer, P.; Rosen, H.; Mumford, R. A.; Springer, M. S. Development of C5a receptor antagonists. Differential loss of functional responses. *J. Immunol.* **1994**, *153*, 4200−4.
(21) Wong, A. K.; Finch, A. M.; Pierens, G. K.; Craik, D.; Taylor, S. M.; Fairlie, D. P. Molecular probes for G-protein coupled receptors. Conformationally constrained antagonists derived from the C-terminus of human plasma protein C5a. *J. Med. Chem.* **1998**, *41*, 3417−22.
(22) Zhang, X.; Boyar, W.; Galakatos, N.; Gonnella, N. C. Solution structure of a unique C5a semi-synthetic antagonist: implications in receptor binding. *Protein Sci.* **1997**, *6*, 65−72.
(23) Pellas, T. C.; Boyar, W.; van Oostrum, J.; Wasvary, J.; Fryer, L. R.; Pastor, G.; Sills, M.; Braunwalder, A.; Yarwood, D. R.; Kramer, R.; Kimble, E.; Hadala, J.; Haston, W.; Moreira-Ludewig, R.; Uziel-Fusi, S.; Peters, P.; Bill, K.; Wennogle, L. P. Novel C5a receptor antagonists regulate neutrophil functions in vitro and in vivo. *J. Immunol.* **1998**, *160*, 5616−21.
(24) Kessler, H. Conformation and biological activity of cyclic peptides. *Angew Chem., Int. Ed.* **1982**, *21*, 512−23.
(25) Dyson, H. J.; Wright, P. E. Defining solution conformations of small linear peptides. *Annu. Rev. Biophys. Chem.* **1991**, *20*, 519−38.
(26) Rose, G. D.; Gierasch, L. M.; Smith, J. A. Turns in peptides and proteins. *Adv. Protein Chem.* **1985**, *37*, 1−109.

(27) Short, A.; Wong, A. K.; Finch, A. M.; Haaima, G.; Shiels, I. A.; Fairlie, D. P.; Taylor, S. M. Effects of a new C5a receptor antagonist on C5a- and endotoxin-induced neutropenia in the rat. *Br. J. Pharmacol.* **1999**, *126*, 551−4.

(28) Abbenante, G.; Fairlie, D. P.; Gahan, L. R.; Hanson, G. R.; Pierens, G. K.; van den Brenk, A. L. Conformational control by thiazole and oxazoline rings in cyclic octapeptides of marine origin. Novel macrocyclic chair and boat conformations. *J. Am. Chem. Soc.* **1996**, *118*, 10384−8.

(29) Pardi, A.; Billeter, M.; Wüthrich, K. Calibration of the angular dependence of the amide proton-C alpha proton coupling constants, 3JHN alpha, in a globular protein. Use of 3JHN alpha for identification of helical secondary structure. *J. Mol. Biol.* **1984**, *180*, 741−51.

(30) Brünger, A. T. *X-PLOR Manual Version 3.1*; Yale University: New Haven, CT, 1992.

(31) Nilges, M.; Gronenborn, A. M.; Brünger, A. T.; Clore, G. M. Determination of three-dimensional structures of proteins by simulated annealing with interproton distance restraints. Application to crambin, potato carboxypeptidase inhibitor and barley serine proteinase inhibitor 2. *Protein Eng.* **1988**, *2*, 27−38.

(32) Clore, G. M.; Brünger, A. T.; Karplus, M.; Gronenborn, A. M. Application of molecular dynamics with interproton distance restraints to three-dimensional protein structure determination. A model study of crambin. *J. Mol. Biol.* **1986**, *191*, 523−51.

(33) Brooks, B. R.; Bruccoleri, R. E.; Olafson, B. D.; States, D. J.; Swaminathan, S.; Karplus, M. CHARMM: A program for macromolecular energy minimization and dynamics calculations. *J. Comput. Chem.* **1983**, *4*, 187−217.